Participation in Negative Capacitance of Diffusion-Controlled Voltammograms of Hemin

ACS OMEGA

http://pubs.acs.org/journal/acsodf

Article

Participation in Negative Capacitance of Diffusion-Controlled Voltammograms of Hemin

Koichi Jeremiah Aoki, Sosuke Taniguchi, and Jingyuan Chen*

Cite This: *ACS Omega* 2020, 5, 29447−29452

Read Online

ACCESS | Metrics & More | Article Recommendations | Supporting Information

ABSTRACT: Hemin in dimethyl sulfoxide solution has exhibited voltammograms controlled by diffusion at glassy carbon electrodes for slow scan rates, although it is adsorbed slightly. In contrast, voltammograms for high scan rates, $\nu > 1$ V s^{-1}, were governed by some kinds of kinetics judging from the scan rate dependence of peaks. The kinetics is close to that of a ferrocenyl derivative, in which the currents include the capacitive component with negative values. The capacitive one can be identified with the proportionality to the scan rates. The variation of the peak currents with ν yielded −200 μF cm^{-2}. This negative value, being associated with the charge transfer reaction, makes cyclic voltammograms deviated downward from the diffusion-controlled behavior, resembling an irreversible reaction of the Butler−Volmer kinetics. Double layer capacitances are generally formed so that the applied electric field may be relaxed. The reduction of hemin forms a dipole coupled with a cation of the salt. The dipole orients from the electrode to the bulk, whereas the solvent dipoles orients in the opposite direction. Therefore, the capacitance is observed negatively. The capacitance determined by ac impedance took also negative values when the applied dc potential was only in the potential domain for the charge transfer. These complications can be avoided in electrocatalysis by use of such slow voltammetry as scan rates of 0.1 V s^{-1} and ac frequency of 0.2 Hz.

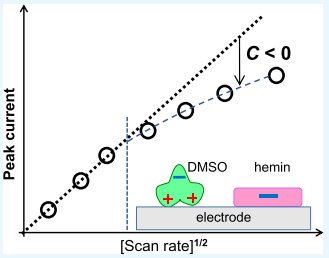

INTRODUCTION

Hemin, known as a natural porphyrinatoiron complex, has been used to catalyze reductively dioxygen and hydrogen peroxide at carbon paste electrodes[1−3] and carbon fiber electrodes.[4] Criteria of the electrocatalysis are enhancement of the reduction currents and/or positively potential shifts from the reduction potential of hemin. They can be utilized if voltammograms of hemin proper are analyzed to determine peaks without ambiguity. Unfortunately, few reaction mechanisms have been clarified quantitatively[5,6] because of adsorption and poor solubility.

Hemin has been demonstrated to be adsorbed on carbon materials,[7−11] as can be found spectroscopically,[12−14] because of the high affinity of porphyrin rings to the graphite structure. However, the adsorption by spectroscopic or visual observation is not necessarily equivalent to the voltammetrically predicted behavior of adsorption. If an electrode adsorbs a redox species so closely packed in monolayer form that the adsorbed density is 10^{-9} mol cm^{-2} or 1 μC mm^{-2}, the adsorbed species is consumed by the faradaic current density, 1 μA mm^{-2}, for 1 s. After the consumption, the redox species is supplied to the electrode from the bulk by diffusion under the adsorbed state. Therefore, the voltammograms are observed to show only the diffusion control except for the initial period. The adsorption information may be revealed in voltammograms at initially short time and/or potential shifts. The hidden complication in voltammograms resembles the irrelevance of microscopic surface roughness of electrodes to diffusion-controlled currents.[15]

We try to predict here the voltammetric behavior of hemin in a wide domain of voltage scan rates, ν. The behavior at slow scan rates may be controlled by diffusion in the bulk without chemical complications, as was discussed above. This has been partially demonstrated.[5,16,17] In contrast, high scan rates may reveal a surface wave of adsorbed hemin, of which the peak current is proportional to ν. They give rise to charging current, which is also proportional to ν. As a result, the observed current may be a sum of the two components proportional to $\nu^{1/2}$ and to ν. However, no adsorption wave has been overlapped with the diffusion current.[5,6] Furthermore, the peak currents were lower than the diffusion-controlled ones associated with peak potential shift,[10,18−21] like in complication by heterogeneous kinetics. This behavior can also be predicted from the capacitive current brought about by the redox reactions.[22−24] It is important to clarify the true rate-determining step in order to clarify electrocatalytic criteria from enhancement of the reduction currents and potential shifts by scan rates. A key is to characterize an effect of adsorption on catalysis quantitatively. The present work aims at solving the complications by fast scan cyclic voltammetry

Received: September 8, 2020
Accepted: October 5, 2020
Published: November 4, 2020

and ac-impedance measurements of hemin in dimethyl sulfoxide at the glassy carbon (GC) electrode and the platinum one.

EXPERIMENTAL SECTION

Dimethyl sulfoxide (DMSO), which was distilled under reduced pressure, was dried with molecular sieves, 3 Å. Hemin (Wako) with nominal 97% purity was stored in a refrigerator. Tetrabutylammonium perchlorate (TBAP) used as salt was dried at 60 °C in an oven for 7 h. All electrochemical experiments were performed in a three-electrode cell including a Pt wire auxiliary electrode and a Ag/Ag^+ reference electrode (0.01 M (M = mol dm^{-3}) $AgNO_3$ + 0.1 M TBAP + DMSO). The working electrode was a platinum wire 0.5 mm in diameter inserted into the hemin solution by a given length (ca. 10 mm). The length was evaluated with an optical microscope. The other working electrode was a glassy carbon (GC) 3 mm in diameter commercially available (BAS). The solution was deaerated with nitrogen gas for 20 min before voltammetry.

A potentiostat used was Compactstat (Ivium, Netherlands) for cyclic voltammetry and ac-impedance measurements. A delay of the potentiostat was examined by using a carbon resistance 1 kΩ for a dummy cell, to which cyclic voltammetry was applied in the voltage domain of 1 V. The maximum difference in the currents for the forward scan from for the reverse scan was 3% at 8 V s^{-1}. Ac impedance was obtained at an ac voltage of 0.01 V in the frequency range from 0.1 Hz to 5 kHz.

RESULTS AND DISCUSSION

Figure 1 shows voltammograms of hemin solution at two scan rates. The waves in the potential range from −0.5 to −0.3 V

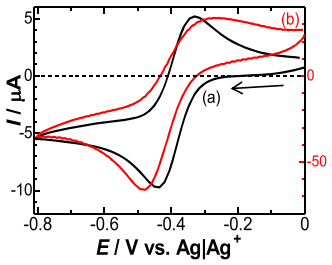

Figure 1. Cyclic voltammograms of 2.4 mM hemin + 0.15 M TBAP + DMSO solution at the Pt electrode for (a) ν = 0.01 V s^{-1} (in the left axis) and (b) ν = 1.0 V s^{-1} (in the right axis). The arrow means the direction of the potential scan.

can be attributed to the redox reaction of hemin.[5,6] Not only the shape of the voltammograms (Figure 1a) but also the difference (0.10 V) in the peak-to-peak potential at low scan rates seems to suggest the diffusion-controlled step (0.06 V). However, the voltammetric shape for oxidation at high scan rates (Figure 1b) had a round peak, implying a diffusion-like process with complications.

Figure 2 shows variations of the peak currents, I_p, at the Pt electrode with the square roots of the scan rates in order to examine whether the current may be controlled by diffusion. The proportionality of I_p for ν < 0.15 V s^{-1} to $\nu^{1/2}$ suggests the diffusion control. The slope of the proportionality for the reduction peak current enabled us to estimate the diffusion coefficient, 1.1 × 10^{-6} cm^2 s^{-1}. This value corresponds to a

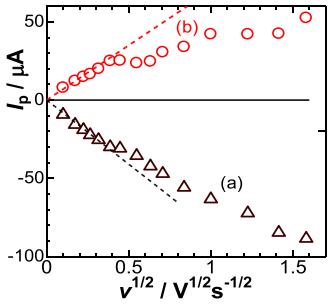

Figure 2. Variations of the (a) reduction and (b) oxidation peak currents with the square roots of the scan rates at the Pt electrode in 2.4 mM hemin + 0.15 M TBAP + DMSO solution.

molecule 1.6 nm diameter in DMSO solution by the Stokes–Einstein equation for the viscosity of DMSO at 20 °C. From the ratio (0.9) of the slope for the oxidation currents to that for the reduction one in magnitude, the diffusion coefficient of reduced hemin is smaller than that of hemin by 0.8 times. This fact indicates that the reduced hemin should be solvated to increase the hydrodynamic diameter. Almost the same behavior as the above was obtained at the GC electrode. Therefore, there was no proof of a surface wave by adsorption even at the GC electrode. For scan rates higher than 0.15 V s^{-1}, the plots deviated lower from the proportionality. If faradaic reactions of adsorbed hemin would bring about a surface wave being proportional to ν, the plots might deviate upward from the proportional line in Figure 2. The lower deviation indicates that adsorbed hemin should not contribute to the voltammograms.

In order to demonstrate participation in the adsorption, we measured voltammograms in the TBAP + DMSO solution at the electrodes that were immersed into the hemin solution for 2 h in advance. Figure 3 shows the voltammograms at the (a)

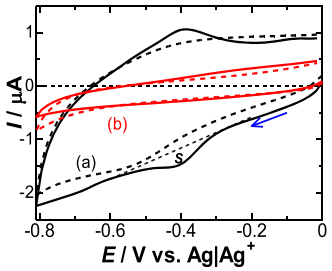

Figure 3. Linear sweep voltammograms in 0.15 M TBAP + DMSO solution at (a) the GC electrode and (b) the Pt electrode for ν = 0.1 V s^{-1} obtained after immersing the electrodes into hemin + DMSO solution for 2 h.

GC electrode and (b) Pt electrode before (dashed curves) and after (solid curves) the immersion. The voltammograms take a frequently observed capacitive shape. Currents at −0.2 V were proportional to the scan rates less than 0.2 V s^{-1}. The slopes provided values of the double layer capacitance, 90 and 20 μF cm^{-2}, for the GC and the Pt electrode respectively. The Pt electrode showed the overlapped voltammograms, indicating unrecognized adsorption. In contrast, the GC exhibited the reduction and the oxidation waves of hemin after the immersion. Therefore, the GC adsorbs hemin. The area, denoted as S in Figure 3a, at the reduction wave at −0.4 V shows the charge density of ca. 10^{-10} mol cm^{-2}, suggesting monolayer adsorption.[6,25] A possible reason of the adsorption

https://dx.doi.org/10.1021/acsomega.0c04384
ACS Omega 2020, 5, 29447−29452

of hemin to carbon materials is the high affinity of porphyrin rings to the graphite structure, as found by spectroscopy.[12−14]

We examine the faradaic voltammograms of dissolved hemin at various scan rates rather than adsorbed hemin. Figure 4

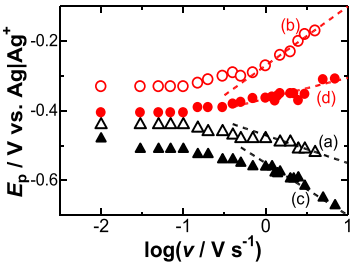

Figure 4. Dependence of (a, c) the reduction and (b, d) the oxidation peak potentials on the logarithmic scan rates at the Pt (a, b) and the GC (c, d) electrodes in 2.4 mM hemin + 0.15 M TBAP + DMSO solution.

shows variations of the peak potential, E_p, with the logarithmic scan rates. The difference in the two peak potentials becomes larger with an increase in the scan rates, as similar to the reported result.[17,26] This type of variations has often been explained in terms of the ohmic loss by solution resistance and sluggishly heterogeneous charge transfer rates. According to the ac-impedance measurements to be described later, the solution resistance was ca. 170 Ω, which yields only 12 mV shift even at I_p = 70 μA (for v = 1 V s^{-1}). Therefore, the solution resistance does not cause such a noticeable peak potential shift as in Figure 4. The other possibility of the peak potential shift is sluggish charge transfer rates,[20] a typical of which is a Butler−Volmer-type irreversible reaction. The theory has stated[19] that peak potentials for irreversible reactions should shift linearly with log v and that the peak current should be proportional to $v^{1/2}$ with the slope less than that of the diffusion-controlled current. On the other hand, our experimental results showed that the peak potentials for v > 0.1 V s^{-1} were shifted linearly with log v for v > 1 V s^{-1} at both the Pt and GC electrodes. The magnitudes of the slopes at the Pt electrode were 80 and 170 mV for the reduction and the oxidation peaks, respectively, whereas those at the GC were 150 and 60 mV. Applying the Butler−Volmer kinetics to these results yields the cathodic and the anodic transfer coefficients, 0.74 and 0.35 for the Pt, respectively, and 0.39 and 0.98 for the GC. The validity of the Butler−Volmer kinetic equation can be verified theoretically not only by the linearity in E_p vs log v plots but also by the unity of the sum of the anodic and the cathodic transfer coefficients. However, the sum of the coefficients for the GC, 1.4, disagrees with the kinetic theory. Furthermore, non-proportionality (zero intercept with a line) of I_p with $v^{1/2}$ for v > 1.0 V s^{-1} in Figure 2 is inconsistent with the theory. Therefore, the current is not controlled by irreversible reactions. Some reports on hemin have explained the shift in terms of the heterogeneous kinetics.[21,26]

The other possibility of both the downward deviation in Figure 2 and the potential shifts in Figure 4 is the participation in the negative capacitance associated with the redox reaction.[22−24,27] It is based on the following concept.[28] When a potential cathodic enough to reduce hemin is applied to the electrode, the electric field near the electrode is directed from the solution to the electrode, as illustrated in Figure 5. Then, dipoles of solvent DMSO, abbreviated as >S$^+$−O$^-$, are

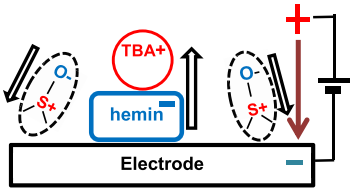

Figure 5. Illustration for orientations of DMSO (>S$^+$−O$^-$) dipoles and a dipole of reduced hemin$^-$ and TBA$^+$ cation by the applied electric field of which the intensity is large enough to reduce hemin.

oriented on the electrode in the direction along the electric field. The orientation works as relaxing the intensity of the field. The negative charge on the reduced hemin is necessarily neutralized by cations, of which the main species is tetrabutylammonium cation (TBA$^+$), to work as an electric dipole. The dipole is oriented from the electrode to the solution, opposite to both the electric field and the DMSO dipoles. When oriented DMSO dipoles show double layer capacitive current by time variation of applied voltage, the dipoles of the reduced hemin should exhibit the opposite sign of the capacitive current so that capacitive values by DMSO are suppressed. Only low concentrations of solvent dipoles can be oriented in the direction of the electric field [30] because of dipole−dipole interactions. If the concentration of hemin is higher than that of the oriented DMSO, the capacitive value by hemin dipoles overcomes that of DMSO in magnitude. Then, the observed capacitive values are measured to be negative.

The observed reduction peak current including the negatively capacitive current is represented by[22]

$$-I_p = 0.446AFc^*(FDv/RT)^{1/2} + C_{rx}v \quad (1)$$

where C_{rx} is the negative capacitance by the redox reaction, A is the geometric area of the electrode, F is the Faraday constant, c^* is the bulk concentration of hemin, D is the diffusion coefficient of hemin in DMSO, R is the gas constant, and T is the temperature. Equation 1 means that $-I_p v^{-1/2}$ should be linear to $v^{1/2}$. Figure 6 shows plots of $-I_p v^{-1/2}$ at (a) the Pt

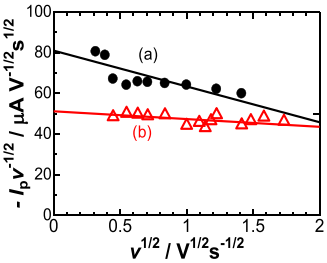

Figure 6. Variations of $-I_p v^{-1/2}$ with $v^{1/2}$ for (a) the Pt electrode and (b) the GC electrode.

electrode and (b) the GC electrode against $v^{1/2}$, exhibiting each line as predicted from eq (1), where the values of the intercept are the same as the slopes of I_p vs $v^{1/2}$ at slow scan rates. The negative slopes imply that the capacitance should be negative, −100 μF cm^{-2} for the Pt electrode and −50 μF cm^{-2} for the GC electrode. The difference in the two values will be discussed in the ac-impedance section. The former value is three times larger than the conventional DLCs.[29,30]

The negative capacitance has been able to be observed accurately with ac impedance.[5,27,31] Real, Z_1, and imaginary parts, Z_2, of ac impedance were measured at the platinum

https://dx.doi.org/10.1021/acsomega.0c04384
ACS Omega 2020, 5, 29447−29452

electrode in the hemin solution at various dc potentials. The Nyquist plots, Z_1 vs $-Z_2$, in the polarized dc-potential domain ($-0.80 < E/\mathrm{V} < -0.48$, $-0.27 < E/\mathrm{V} < 0.0$) fell on a line with a slope of 5.7 ± 0.1 and the intercept on the Z_1 axis, which corresponds to the solution resistance, R_s = 170 Ω in the 0.15 M TBAP + 2.4 mM hemin + DMSO solution. First, we pay attention to the ac current in the polarized potential domain. The definitions of the capacitance in electromagnetics and the time derivative of the charge yield the current density[29]

$$j = \mathrm{d}(CV)/\mathrm{d}t = C(dV/dt) + V(dC/dt) = (i + \lambda)\omega CV \quad (2)$$

for the ac voltage, $V = V_{ac}e^{i\omega t}$, and the power law, $C = C_{1Hz}f^{-\lambda}$, where i is the imaginary unit, ω is the angular rate of ac voltage, f is the ac frequency ($f = \omega/2\pi$), λ is a constant close to 0.1, and C_{1Hz} is the capacitance at f = 1 Hz. Then, the real and the imaginary admittances, defined by $Y = Y_1 + iY_2 = 1/Z$, are represented explicitly as

$$Y_1 = 2\pi\lambda C_{1Hz} f^{1-\lambda} = (Z_1 - R_s)/\{(Z_1 - R_s)^2 + Z_2^2\} \quad (3A)$$

$$Y_2 = 2\pi C_{1Hz} f^{1-\lambda} = -Z_2/\{(Z_1 - R_s)^2 + Z_2^2\} \quad (3B)$$

Logarithmic plots of Y_1 and Y_2 with the frequency exhibit lines, as shown in Figure 7a,b. The slope and the intercept for

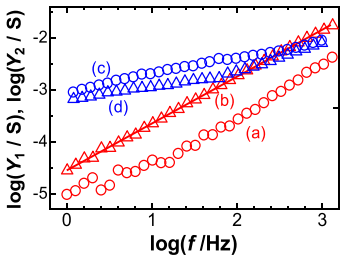

Figure 7. Variations of (a, c) Y_1 and (b, d) Y_2 with the frequency on the logarithmic scale for E_{dc} = (a, b) −0.1 V and (c, d) −0.4 V in 0.15 M TBAP + 2.4 mM hemin + DMSO solution at the Pt electrode. The slope of (b) is 0.903 or λ = 0.097.

the line of Y_2 can evaluate λ and C_{1Hz} more accurately than for Y_1. The higher accuracy of Y_2, which is larger than Y_1 by ca. one order in magnitude, is due to the ac current mainly caused by the capacitance.

When an electrode reduction occurs at a cathodic potential, the generation of a negative charge on the electrode conflicts with the relaxation of the electric field which is brought about by the orientation of solvent dipoles (see Figure 5). This effect blocks the orientation of solvent dipoles so that the observed capacitance decreases. The further decrease makes the observed capacitance take a negative value, especially at high concentrations of the redox species.[27,31] The diffusion-controlled ac impedance caused by redox reaction is expressed by the Warburg impedance, in which the real admittance takes a same value as the imaginary one does. The difference between the two cancels the diffusion component of the admittance, and hence it tends only to the capacitive component. The difference in eq 3 retains only the contribution of the capacitive admittance:

$$Y_2 - Y_1 = 2\pi(1 - \lambda)C_{1Hz} f^{1-\lambda} \quad (4)$$

Figure 7c,d shows the frequency dependence of Y_1 and Y_2 observed in the dc potential (E_{dc}) domain for the faradaic reaction. The finding of $Y_1 > Y_2$ implies that $(1 - \lambda)C_{1Hz}$ should be negative or C_{1Hz} should be. In contrast, we found $Y_1 < Y_2$ or $C_{1Hz} > 0$ in the polarized potential domain (a, b).

Figure 8 shows variations of $\log[-(Y_2 - Y_1)]$ with $\log f$ for three values of E_{dc} in the potential domain for the faradaic

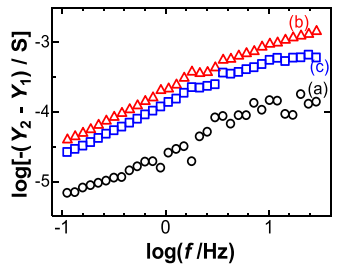

Figure 8. Variations of $-(Y_2 - Y_1)$ with the frequency on the logarithmic scale for E_{dc} = (a) −0.45 V, (b) −0.40 V, and (c) −0.35 V.

reaction. The plots fall on each line, of which the slope and the intercept provide λ and C_{1Hz}, respectively. The intercept values become large as the dc potential tends to the standard potential of hemin. Figure 9 shows the dependence of the

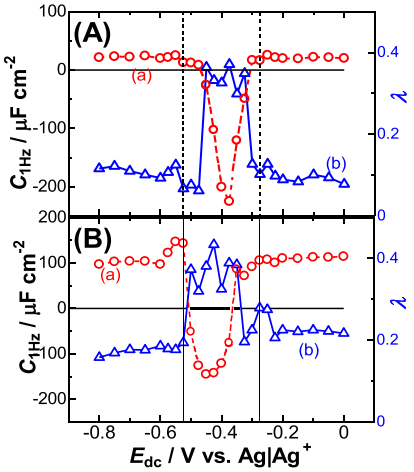

Figure 9. Dependence of C_{1Hz} and λ on E_{dc} at (A) the Pt electrode and (B) the GC electrode.

determined C_{1Hz} and λ on E_{dc} at (A) the Pt electrode and (B) the GC electrode. C_{1Hz} in the reacting potential domain ($-0.45 < E_{dc}/\mathrm{V} < -0.30$) takes negative values, whereas it remains almost a constant close to the conventional values of the DLCs (22 μF cm^{-2} at the Pt electrode and 100 μF cm^{-2} at the GC electrode) in the polarized domain. These potential domains should be compared with those of the voltammograms in Figure 1. The increase of λ in the reacting domain implies that the frequency dispersion should be strong or that the generated charge in hemin molecules should be fluctuated by diffusion toward the solution bulk. The minimum values of C_{1Hz} were ca. −220 at the Pt electrode and −150 μF cm^{-2} at the GC electrode. The differences between the minimum C_{1Hz} and the DLC value are (22 + 220) μF cm^{-2} at the Pt electrode and (100 + 150) μF cm^{-2} at the GC electrode. The common value (250) indicates that it cannot be attributed to properties of DLCs depending on surface porosity or roughness but should be caused by diffusion currents independent of the porosity or the roughness.[15]

https://dx.doi.org/10.1021/acsomega.0c04384
ACS Omega 2020, 5, 29447−29452

We summarize several capacitive values in Table 1, through which we can discuss effects of the capacitance on electrode

Table 1. Several Values of Capacitances at the Two Electrodes by the Two Methods

	DLC (μF cm^{-2})		C_{rx} (μF cm^{-2})	
electrode	AC	CV	AC	CV
Pt	22	20	−200	−100
GC	100	90	−200	−50

materials and the electrochemical methods. The value of the DLC at the GC electrode was three times larger than that at the Pt electrode, probably because of pores of the GC surface, which works as adsorption of hemin. In contrast, the negative capacitance is caused by the faradaic currents, and hence it depends only on the diffusion current rather than the microscopic surface structure of the electrodes. As a result, the value of C_{rx} by the ac impedance is common for the Pt electrode and the GC electrode. On the other hands, values of C_{rx} by CV depend on the kinds of electrode materials because they include values of DLC owing to coupling of the time dependence with the potential dependence. Especially, the latter is significant when the scanned voltage domain is wide as used for current control in charging-discharging processes.[27]

CONCLUSIONS

Voltammograms of hemin in DMSO solution exhibited diffusion-controlled currents both at the GC and Pt electrodes although adsorption of hemin at the GC electrode is detected voltammetrically as mono-molecular adsorption. The diffusion control is not contradicted with the adsorption the observed current is independent of the amount of adsorbed hemin on the electrode. The difference in the controlling steps, i.e., the diffusion being proportional to $v^{1/2}$ while adsorption being to v, generally makes adsorption waves prominent at fast scans. However, fast scans suppress the current by the amount of proportional to v. This can be attributed to the negative capacitance caused by the reduction of hemin in solution, which gives rise to peak potential shift and the lower deviation from the proportionality of the peak current to $v^{1/2}$. The negative capacitance can be demonstrated to be caused by the faradaic reaction because of the observation only in the potential domain of the redox reaction. The values of the negative capacitance are common to the Pt and the GC at a given value of the diffusion current, whereas the two kinds of the electrodes exhibit individual values of the DLCs. The potential shifts and the deviation of the peak current from the proportionality are nonessential to reaction mechanisms of hemin but belong to an inevitable observation associated with data acquisition at a short time.

The negative capacitance caused by charge transfer reduction is responsible for the formation of negative redox charge on an electrode. The formation enhances the electric field in the electric double layer, although the field should be decreased in nature by bringing about DLCs. As a result, it causes capacitive current in the direction opposite to the current through the DLCs. This is observed as a negative capacitance. This concept seems reconstruction of ions at double layers, but there is no reconstruction of molecules or charges.

ASSOCIATED CONTENT

Supporting Information

The Supporting Information is available free of charge at https://pubs.acs.org/doi/10.1021/acsomega.0c04384.

(PPTX)

AUTHOR INFORMATION

Corresponding Author

Jingyuan Chen − *Department of Applied Physics, University of Fukui, Fukui 910-0017, Japan;* orcid.org/0000-0002-5042-6179; Email: jchen@u-fukui.ac.jp

Authors

Koichi Jeremiah Aoki − *Electrochemistry Museum, Fukui 910-0804, Japan*

Sosuke Taniguchi − *Department of Applied Physics, University of Fukui, Fukui 910-0017, Japan*

Complete contact information is available at: https://pubs.acs.org/10.1021/acsomega.0c04384

Notes

The authors declare no competing financial interest.

REFERENCES

(1) Brezina, M. Elektrodenprozesse von Sauerstoff und Wasserstoffperoxid an Platin, Silber und Kohlenstoff. *Ber. Bunsen Gesellschaft.* **1973**, *77*, 849−852.

(2) Březina, M.; Hofmanová-Matějková, A. Study of the reduction of oxygen on a carbon paste electrode in an alkaline medium. *Collect. Czech. Chem. Commun.* **1973**, *38*, 3024−3031.

(3) Zheng, N.; Zeng, Y.; Osborne, P. G.; Li, Y.; Chang, W.; Wang, Z. Electrocatalytic reduction of dioxygen on hemin based carbon paste electrode. *J. Appl. Electrochem.* **2002**, *32*, 129−133.

(4) Antoniadou, S.; Jannakoudakis, A. D.; Theodoridou, E. Electrocatalytic reactions on carbon fibre electrodes modified by hemine I. Electroreduction of oxygen. *Synth. Met.* **1989**, *30*, 283−294.

(5) Aoki, K. J.; Li, W.; Chen, J.; Nishiumi, T. Irreversibility of catalytic reduction of dioxygen by dissolved hemin. *J. Electroanal. Chem.* **2014**, *713*, 131−135.

(6) Li, W.; Aoki, K. J.; Chen, J.; Nishiumi, T. Conditions of predominant occurrence of catalytic reduction of O2 by ferrous hemin over formation of ferrous hemin-O2 adduct. *J. Electroanal. Chem.* **2015**, *743*, 134−138.

(7) Bianco, P.; Haladjian, J.; Draoui, K. Electrochemistry at a pyrolytic graphite electrode: Study of the adsorption of hemin. *J. Electroanal. Chem.* **1990**, *279*, 305−314.

(8) Kannan, B.; Kumsa, D.; Jebaraj, A. J.; Méndez-Albores, A.; Georgescu, N. S.; Scherson, D. The electrocatalytic properties of adsorbed hemin and its nitrosyl adduct on glassy carbon surfaces toward hydroxylamine in aqueous neutral electrolytes. *J. Electroanal. Chem.* **2017**, *793*, 250−256.

(9) de Groot, M. T.; Merkx, M.; Wonders, A. H.; Koper, M. T. M. Electrochemical Reduction of NO by Hemin Adsorbed at Pyrolitic Graphite. *J. Am. Chem. Soc.* **2005**, *127*, 7579−7586.

(10) Wang, Y.; Hosono, T.; Hasebe, Y. Hemin-adsorbed carbon felt for sensitive and rapid flow-amperometric detection of dissolved oxygen. *Microchim. Acta* **2013**, *180*, 1295−1302.

(11) Huang, W.; Hao, Q.; Lei, W.; Wu, L.; Xia, X. Polypyrrole-hemin-reduce graphene oxide: rapid synthesis and enhanced electrocatalytic activity towards the reduction of hydrogen peroxide. *Mater. Res. Express* **2014**, *1*, No. 045601.

(12) Lv, X.; Weng, J. Ternary Composite of Hemin, Gold Nanoparticles and Graphene for Highly Efficient Decomposition of Hydrogen Peroxide. *Sci. Rep.* **2013**, *3*, 3285.

(13) Cai, W.-B.; Stefan, I. C.; Scherson, D. A. Determination of adsorption isotherm of species adsorbed on roughened silver

electrodes from in situ quantitative surface enhanced Raman spectroscopy. *J. Electroanal. Chem.* **2002**, *524-525*, 36−42.
(14) Hu, W.; Yu, X.; Hu, Q.; Kong, J.; Li, L.; Zhang, X. Methyl Orange removal by a novel PEI-AuNPs-hemin nanocomposite. *J. Environ. Sci.* **2017**, *53*, 278−283.
(15) Popov, K. I.; Nikolić, N. D.; Živković, P. M.; Branković, G. The effect of the electrode surface roughness at low level of coarseness on the polarization characteristics of electrochemical processes. *Electrochim. Acta* **2010**, *55*, 1919−1925.
(16) Zhang, H.; Aoki, K.; Chen, J.; Nishiumi, T.; Toda, H.; Torita, E. Voltammetric determination of both concentration and diffusion coefficient by combinational use of regular and micro electrodes. *Electroanalysis* **2011**, *23*, 947−952.
(17) Samajdar, R. N.; Manogaran, D.; Yashonath, S.; Bhattacharyya, A. J. Using porphyrin−amino acid pairs to model. *Phys. Chem. Chem. Phys.* **2018**, *20*, 10018−10029.
(18) Chen, J.; Wollenberger, U.; Lisdat, F.; Ge, B.; Scheller, F. W. Superoxide sensor based on hemin modified electrode. *Sens. Actuat. B* **2000**, *70*, 115−120.
(19) Matsuda, H.; Ayabe, Y. The theory of the cathode-ray polarography of Randles-Sevcik. *Z. Elektrochmie.* **1955**, *59*, 494−503.
(20) Bard, A. J.; Faulkner, L. R. *Electrochemical Methods: Fundamentals and applications*, 2nd ed.; Wiley: New York, 2001, pp. 234−239.
(21) Compton, D. L.; Laszlo, J. A. Direct electrochemical reduction of hemin in imidazolium-based ionic liquids. *J. Electroanal. Chem.* **2002**, *520*, 71−78.
(22) Aoki, K. J.; Chen, J.; Liu, Y.; Jia, B. Peak potential shift for fast cyclic voltammograms owing to capacitance of redox reactions. *J. Electroanal. Chem.* **2020**, *856*, 113609.
(23) Tang, P.; Aoki, K. J.; Chen, J. Reduction Charge Smaller than the Deposited One in Cathodic Stripping Voltammograms of AgCl. *Am. J. Anal. Chem.* **2019**, *10*, 286−295 http://www.scirp.org/journal/ajac.
(24) Aoki, K. J.; Chen, J.; Wang, R. Stripped Charge of Ag less than Deposited one Owing to Negative Capacitance Caused by Redox Reactions. *Electroanalysis* **2019**, *31*, 1−2310.
(25) Aoki, K. J.; Li, W.; Chen, J.; Nishiumi, T. Irreversibility of catalytic reduction of dioxygen by dissolved hemin. *J. Electroanal. Chem.* **2014**, *713*, 131−135.
(26) Ma, Q.; Ai, S.; Yin, H.; Chen, Q.; Tang, T. Towards the conception of an amperometric sensor of l-tyrosine based on Hemin/PAMAM/MWCNT modified glassy carbon electrode. *Electrochim. Acta* **2010**, *55*, 6687−6694.
(27) Aoki, K. J.; Chen, J.; Tang, P. Capacitive currents flowing in the direction opposite to redox currents. *J. Phys. Chem. C* **2018**, *122*, 16727−16732.
(28) Aoki, K. J.; Chen, J. Effects of the dipolar double layer on elemental electrode processes at micro- and macro-interfaces. *Faraday Discuss.* **2018**, *210*, 219−234.
(29) Hou, Y.; Aoki, K. J.; Chen, J.; Nishiumi, T. Invariance of double layer capacitance to polarized potential in halide solutions. *Univers. J. Chem.* **2013**, 162−169.
(30) Hou, Y.; Aoki, K. J.; Chen, J.; Nishiumi, T. Solvent Variables Controlling Electric Double Layer Capacitance at Metal|Solution Interface. *J. Phys. Chem. C* **2014**, *118*, 10153−10158.
(31) Aoki, K. J.; Chen, J.; Zeng, X.; Wang, Z. Decrease in double layer capacitance by Faradaic current. *RSC Adv.* **2017**, *7*, 22501−22501.

https://dx.doi.org/10.1021/acsomega.0c04384
ACS Omega 2020, 5, 29447−29452